TISSUE ENGINEERING: Part C
Volume 16, Number 5, 2010

DOI: 10.1089/ten.tec.2009.0759

Synchrotron X-Ray Bioimaging of Bone Regeneration by Artificial Bone Substitute of MegaGen Synthetic Bone and Hyaluronate Hydrogels

Junseok Yeom, M.Eng.,[1,*] Soeun Chang, M.Eng.,[1,*] Jung Kyu Park, M.Eng.,[1] Jung Ho Je, Ph.D.,[1] Dong Jun Yang, M.Eng.,[2] Seok Kyu Choi, Ph.D.,[2] Hong-In Shin, Ph.D.,[3] Seung-Jae Lee, Ph.D.,[4] Jin-Hyung Shim, M.Eng.,[4] Dong-Woo Cho, Ph.D.,[4] and Sei Kwang Hahn, Ph.D.[1]

Synchrotron X-ray bioimaging was successfully carried out to observe bone regeneration by a novel artificial bone substitute of bioactive MegaGen Synthetic Bone (MGSB) and hyaluronate (HA) hydrogels. A biphasic calcium phosphate of MGSB was prepared by chemical precipitation method, with a porous spherical morphology. On the basis of the fact that HA plays important roles in bone regeneration and promotes the differentiation, vascularization, and migration of stem cells, HA-cystamine (CYS) hydrogels with cleavable disulfide linkages were prepared to supply HA continuously for effective bone regeneration by their controlled degradation *in vivo*. Among seven different samples using Bio-OSS®, MGSB, and/or several kinds of HA hydrogels, MGSB/HA-CYS hydrogels resulted in the most significant bone regeneration in the calvarial critical bone defect of New Zealand white rabbits. Histological and histomorphometric analyses revealed that the bone regeneration by MGSB/HA-CYS hydrogels was as high as 43%, occupying 71% of the bone defect area with MGSB in the form of a calvarial bone plate in 4 weeks. After that, MGSB was bioabsorbed and replaced gradually with regenerated bones as observed in 8 weeks. Synchrotron X-ray imaging clearly confirmed the effective bone regeneration by MGSB/HA-CYS hydrogels, showing three-dimensional micron-scale morphologies of regenerated bones interconnected with MGSB. In addition, sequential nondestructive synchrotron X-ray tomographic analysis results from anterior to posterior of the samples were well matched with the histomorphometric analysis results. The clinically feasible artificial bone substitutes of MGSB/HA-CYS hydrogels will be investigated further for various bone tissue engineering applications using the synchrotron X-ray bioimaging systems.

Introduction

Bone is a microcomposite of hydroxyapatite crystallites and collagen-rich organic materials.[1] There have been worldwide research efforts for bone tissue engineering.[2–6] Various artificial bone substitutes have been designed and developed for rapid and efficient bone regeneration in clinical applications.[1,6,7] Bio-OSS® is a widely used bovine organic bone substitute. Despite its wide applications, bone regeneration is very slow and the slow resorption causes an invasion of fibroblast.[6] To stimulate the differentiation of osteogenic precursors, osteogenic growth factors, such as bone morphogenic protein (BMP), have been used together with bone substitutes.[2,3,8] Further, mesenchymal stem cells (MSCs) were also encapsulated within hybrid bone substitutes differentiating to osteoblasts for rapid and effective bone regeneration.[4,5,9,10] However, there are many obstacles for these systems to be commercialized for clinical applications because of the high production cost of BMP, the safety issues of MSCs, and so on. Instead of these complicated systems, we tried to develop a novel hybrid bone substitute composed of a biphasic calcium phosphate (BCP) and hyaluronate (HA) hydrogels, taking advantage of angiogenic, osteogenic, and osteoconductive HA.[11–14]

HA is a biodegradable, biocompatible, nonimmunogenic, and natural linear polysaccharide. HA is the only nonsulfated glycosaminoglycan that is abundant in synovial fluid and extracellular matrix.[15] The molecular weight (MW)

[1]Department of Material Science and Engineering, Pohang University of Science and Technology (POSTECH), Pohang, Korea.
[2]MegaGen Research Institute of Science and Technology, Kyeongsan, Korea.
[3]Department of Oral Pathology, School of Dentistry, IHBR, Kyungpook National University, Daegu, Korea.
[4]Department of Mechanical Engineering, Pohang University of Science and Technology (POSTECH), Pohang, Korea.
*These two authors contributed equally to this work.

of HA ranges from several thousands to over millions daltons. Depending on the MW, HA has different physiological roles in the body. Especially, when HA degrades to specific sizes of 3–10 repeating units, it promotes the differentiation, vascularization, and migration of stem cells.[16,17] With a short half-life of several hours in the body, HA is also known to be osteogenic and promotes cell proliferation.[14,15] Accordingly, HA hydrogels were designed to supply HA by their controlled degradation *in vivo* for continuous vascularization or migration of osteoblasts for effective bone regeneration.[18–21] We previously reported the controlled degradation of HA hydrogels to modulate and extend their residence times in the body.[22,23] HA hydrogels containing disulfide bonds degraded almost completely within 1–2 months. The degradation kinetics of HA hydrogels in the body could be controlled more easily by changing the crosslinker than the crosslinking density.[22,23]

In this work, a novel artificial bone substitute composed of MegaGen Synthetic Bone (MGSB) and HA hydrogels was developed for bone tissue engineering applications. A bioactive BCP of MGSB was prepared with a composition of 60 wt% hydroxyapatite and 40 wt% β-tricalcium phosphate (β-TCP). HA-cystamine (CYS) hydrogels with cleavable disulfide linkages were newly synthesized and compared with adipic acid dihydrazide-grafted HA (HA-ADH) hydrogels and HA-divinyl sulfone (DVS) hydrogels with different degradation kinetics. Seven different samples of a control, Bio-OSS, MGSB, Bio-OSS/HA-ADH hydrogels, Bio-OSS/HA-DVS hydrogels, Bio-OSS/HA-CYS hydrogels, and MGSB/HA-CYS hydrogels were implanted in the calvarial critical-sized bone defects in the skulls of New Zealand white male rabbits. Bone regeneration was assessed by histological and histomorphometric analyses after hematoxylin and eosin (H&E) staining in 4 and 8 weeks. Further, X-ray bioimaging was carried out to assess and observe the bone regeneration by the artificial bone substitutes using synchrotron hard X-rays available at the Pohang Light Source (7B2 beamline, Pohang, Korea).[24,25]

Materials and Methods

Materials

Sodium hyaluronate (HA), sodium salt of hyaluronic acid, with a MW of 234 kDa was purchased from Lifecore (Chaska, MN). Bis(sulfosuccinimidyl)suberate (BS^3), 1-ethyl-3-[3-(dimethylamino)propyl]carbodiimide (EDC), phosphate-buffered saline (PBS) tablet, H&E, glutathione, and hyaluronidase from *Streptomyces hyalurolyticus* were purchased from Sigma-Aldrich (St. Louis, MO). ADH, DVS, and CYS dihydrochloride were purchased from Tokyo Chemical Industry (Tokyo, Japan). Hydrochloric acid, sodium hydroxide, methanol, and 1-hydroxybenzotriazole monohydrate (HOBt) were obtained from Wako Pure Chemical Industries (Osaka, Japan). Bio-OSS was obtained from Geistlich Biomaterials (Wulhusen, Switzerland).

Synthesis of MGSB

A BCP of MGSB was prepared by the chemical precipitation method using calcium nitrate tetrahydrate [$Ca(NO_3)_2 \cdot 4H_2O$] and ammonium phosphate dibasic [$(NH_4)_2HPO_4$] as reported elsewhere.[26–28] The composition was optimized to be 60 wt% of hydroxyapatite and 40 wt% of β-TCP for bone tissue engineering applications. The mean particle size and particle size distribution of more than 20 samples were analyzed by scanning electron microscopy.

Synthesis of HA-ADH hydrogels

HA-ADH with approximately 70 mol% of ADH content was prepared as described elsewhere.[22,23] HA-ADH was dissolved in PBS (0.01 M, pH 7.4, at 25°C) for 2 h. As a specific crosslinker to hydrazide, BS^3 was also dissolved in PBS, which was added to the HA-ADH solution. The amount of added BS^3 was 20 mol% of hydrazide groups in HA-ADH. The final precursor solution was mixed and incubated at 37°C for 1 h to complete the crosslinking reaction for HA-ADH hydrogel preparation. Then the HA-ADH hydrogels were sealed within prewashed dialysis membrane tube (molecular weight cut-off [MWCO] of 7 kDa) and dialyzed against excess amount of PBS for 24 h to remove the remaining BS^3.

Synthesis of HA-DVS hydrogels

HA was dissolved in 0.2 N sodium hydroxide (pH = 13). After complete dissolution, DVS was added to the HA solution for the crosslinking reaction with hydroxyl groups of HA.[22,23] The molar ratio of DVS to HA repeating units was 1:1. The final precursor solution was mixed and incubated at 37°C for 1 h to complete the crosslinking reaction for HA-DVS hydrogel preparation. Then the HA-DVS hydrogels were sealed within prewashed dialysis membrane tube (MWCO of 7 kDa) and dialyzed against PBS for 24 h. Na^+ and OH^- ions diffused out though the dialysis membrane neutralizing the pH inside the HA-DVS hydrogels.

Synthesis of HA-CYS hydrogels

HA was dissolved in PBS (0.01 M, pH 7.4) and CYS was added to the HA solution. The amount of CYS was 20 mol% of HA repeating units. EDC and HOBt, which activate the carboxyl groups of HA, were dissolved in PBS and added to the mixed solution of HA and CYS for HA-CYS hydrogel preparation. The molar amount of EDC and HOBt was two times of HA repeating units, respectively. The final precursor solution was mixed and incubated at 37°C for 1 h to complete the crosslinking reaction for HA-CYS hydrogel preparation. Then the HA-CYS hydrogels were sealed within prewashed dialysis membrane tube (MWCO of 7 kDa) and dialyzed against excess amount of PBS for 24 h to remove the remaining EDC, HOBt, and CYS.

In vitro *degradation tests of HA hydrogels*

Three kinds of HA hydrogel samples described above were prepared in syringes for *in vitro* degradation tests.[22,23] Each of HA-ADH hydrogel, HA-DVS hydrogel, and HA-CYS hydrogel was put into a vial, respectively. Then sodium phosphate buffer (0.2 M, pH = 6.2) containing 50 U of hyaluronidase or 100 mM of glutathione was added to the vials. The samples were incubated at 37°C for the predetermined times (0–48 h). After that, the supernatant was completely removed and the remaining weight of HA hydrogels was measured with a balance. The degree of HA hydrogel degradation was represented by a weight ratio (%) of the remaining

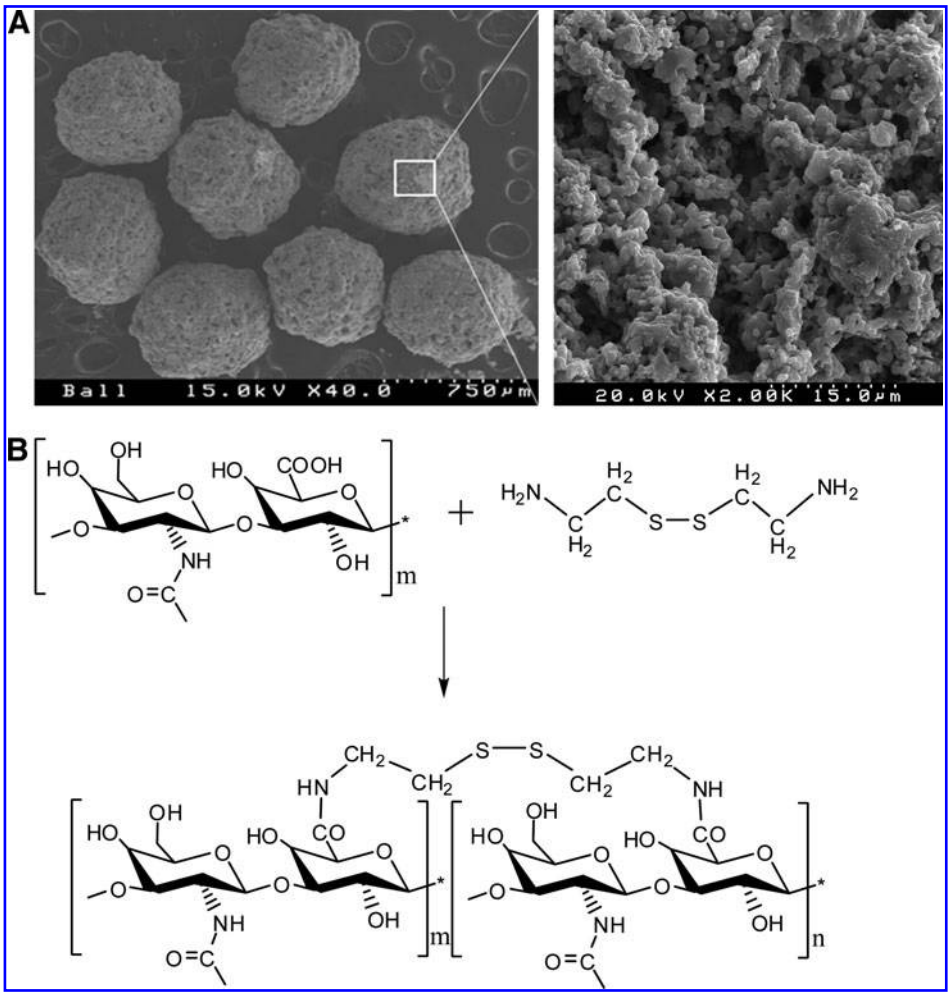

FIG. 1. Artificial bone substitute of MegaGen Synthetic Bone (MGSB) and hyaluronate–cystamine (HA-CYS) hydrogels. (**A**) Scanning electron microscopic image of a biphasic calcium phosphate of MGSB. (**B**) Schematic representation for the preparation of HA-CYS hydrogels.

hydrogel to the original hydrogel. Three replicates were carried out for each sample.

In vivo *bone regeneration tests*

New Zealand white male rabbits weighing about 4 kg were anesthetized by intramuscular injection of zoletil and rompun (v/v = 1/1, 0.1 cc/kg). The scalp of each rabbit was incised and two bone defects with a diameter of 9 mm were made with a trephine bur ($d = 8$ mm). Each of three kinds of HA hydrogels described above was mixed with PBS at a volume ratio of 1:1. The HA hydrogels were completely homogenized to microhydrogels with a homogenizer (T-18 basic; IKA, Tokyo, Japan) at 8000 rpm for 5 min. The prepared HA microhydrogels were mixed with Bio-OSS or MGSB, which were inserted into the calvarial critical-sized bone defects. The amounts of bone grafts and HA hydrogels were 40 mg and 100 µL, respectively. For comparison, the bone defects were also filled with Bio-OSS and MGSB or remained without graft as a nongrafted control. The rabbits were sacrificed for histological and histomorphometric analyses after H&E staining ($n = 3$ for each sample) in 4 and 8 weeks. The regenerated bone defect samples were fixed with 10% formalin for 2 days and decalcified with 10% ethylenediaminetetraacetic acid for 2–3 weeks. The 5-µm-thick paraffin sections were prepared following the routine procedure. The degree of bone regeneration was assessed by observation with a digital camera-connected light microscope (Olympus, Tokyo, Japan) at magnifications of 20× and 100×. Histomorphometric data were collected using a picture analysis program (*i*MT image analysis software; *i*MTechnology, Daejeon, Korea). The percentage of new bone formation was presented as the ratio of new bone area versus total defect area. In addition, the percentage of bioabsorbed MGSB was presented as the ratio of MGSB area in 8 weeks versus that with a negligible biodegradation in 2 weeks. We complied with the institutional ethical use protocols for animals.

Synchrotron X-ray microtomography

Microtomography was performed on the International Consortium of Phase Contrast Imaging and Radiology 7B2 synchrotron X-ray microscopic high flux beamline at the Pohang Light Source.[24,25] The experimental geometry and the detector position in particular were selected to emphasize the refraction-based mechanism. The regenerated bone sample was typically placed 200–400 mm from the detector to achieve the best contrast. The sample was mounted on a high-precision motor-controlled stage with rotational, tilting, and translational resolutions of 0.002°, 0.0009°, and 250 nm, respectively. After passing through the sample, the transmitted X-ray beam was converted by a scintillator to visible light, reflected by a silicon wafer, and then magnified by an optical lens. The detector system consisted of a thin $CdWO_4$

cleaved single crystal ($30\times30\times0.3\,mm^3$; Nihon Kessho Koogaku, Gunma, Japan) scintillator and a charge-coupled device (CCD) camera. A microscope objective lens magnified the image displayed on the scintillator. Then the image was captured by the CCD camera and image acquisition system. Several images were averaged into one image at every 0.9° increment of rotation. This process was repeated 200 times and took less than 1 h. The field of view was tunable by adapting different magnification lens with 1600×1200 pixels. The image set was reconstructed by four parallel computers equipped with a reconstruction algorithm. The reconstructed slices composed of 1600×1600 pixels in the x and y dimensions. Vertically stacked two-dimensional (2D) slices were reconstructed into volume-rendered three-dimensional (3D) images using Amira software. The void volumes after bone regeneration in the bone defect regions were determined by the analysis of 2D tomographic transmission images from anterior to posterior of the samples.

Statistical analysis

The data are expressed as mean ± standard deviation from three separate experiments. Statistical analysis was carried out via *t*-test using a software of SigmaPlot 9.0 and a value for $p < 0.05$ was considered to be statistically significant.

Results

Preparation and characterization of artificial bone substitute

A novel hybrid bone substitute was successfully developed using a bioactive BCP of MGSB and HA hydrogels. MGSB was prepared by the chemical precipitation method to have a composition of 60 wt% of hydroxyapatite and 40 wt% of β-TCP. MGSB had a uniform porous spherical morphology in the particle size range of 500–700 μm, with a mean value of approximately 600 μm, as shown in Figure 1. On the other hand, based on the fact that HA plays important roles in bone regeneration and promotes the differentiation, vascularization, and migration of stem cells, HA-CYS hydrogels with cleavable disulfide bonds were prepared for bone tissue engineering applications. HA-CYS hydrogels were newly synthesized by the crosslinking of HA-COOH with CYS after activation with EDC and HOBt (Fig. 1). *In vitro* degradation of HA-CYS hydrogels was assessed in comparison with HA-DVS hydrogels and HA-ADH hydrogels after treatment with hyaluronidase or glutathione. As shown in Figure 2A, HA-CYS hydrogels and HA-DVS hydrogels degraded completely in 36 h, whereas HA-ADH hydrogels degraded only partially in 48 h. Interestingly, HA-CYS hydrogels with cleavable disulfide bonds also degraded by glutathione (Fig. 2B). HA-CYS hydrogels swelled with increasing degradation and resulted in complete degradation in 36 h. In contrast, HA-ADH and HA-DVS hydrogels did not degrade but swelled in the presence of glutathione (Fig. 2B). The swelling ratio of HA-DVS hydrogels with unmodified carboxyl groups was significantly higher than those of other HA hydrogels. On the basis of *in vitro* degradation test results, HA-CYS hydrogels were micronized with a homogenizer, mixed with a synthetic bone graft of MGSB, and assessed as a novel artificial bone substitute after implantation to the calvarial critical-sized bone defects of New Zealand white rabbits.

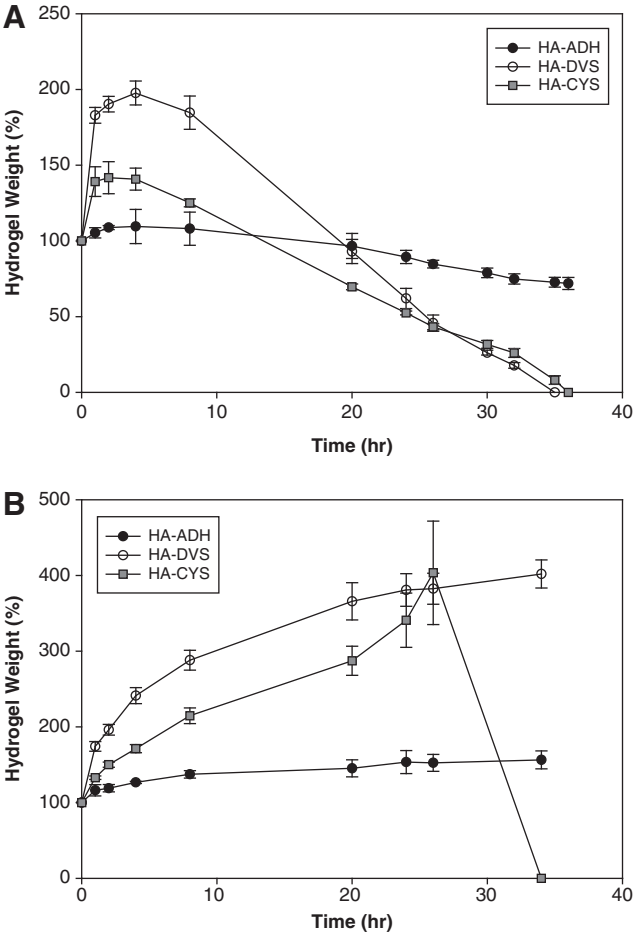

FIG. 2. *In vitro* degradation of adipic acid dihydrazide-modified hyaluronate (HA-ADH, filled circles) hydrogels, HA hydrogels crosslinked with divinyl sulfone (HA-DVS, open circles), and HA hydrogels crosslinked with CYS (HA-CYS, blue squares) after activation with 1-ethyl-3-[3-(dimethylamino)propyl] carbodiimide and 1-hydroxybenzotriazole monohydrate by the treatments with (**A**) hyaluronidase (50 units) from *Streptomyces hyalurolyticus* and (**B**) glutathione (100 mM).

In vivo *bone regeneration by artificial bone substitutes*

The effect of MGSB on bone regeneration was compared with those of the control and a widely used organic bone substitute of Bio-OSS. Figure 3 shows the histological photomicrographic images of calvarial critical-sized bone defects after bone regeneration for 4 weeks. The bone regeneration by the control was not significant in the calvarial bone defect (Fig. 3A). In case of Bio-OSS, an incomplete bone plate composed of regenerated bone and retained bone substitutes was formed, but the regenerated bone was not tightly integrated with Bio-OSS (Fig. 3B). Although MGSB did not also form a complete calvarial bone plate in 4 weeks, the newly formed bone was well integrated to the MGSB with a better degree of bone regeneration than Bio-OSS (Fig. 3C). To provide osteogenic, osteoconductive, and angiogenic HA continuously during bone regeneration, HA-CYS hydrogels with cleavable disulfide bonds were prepared and mixed with Bio-OSS or MGSB, which were implanted in the calvarial critical-sized bone defects of New Zealand white rabbits.

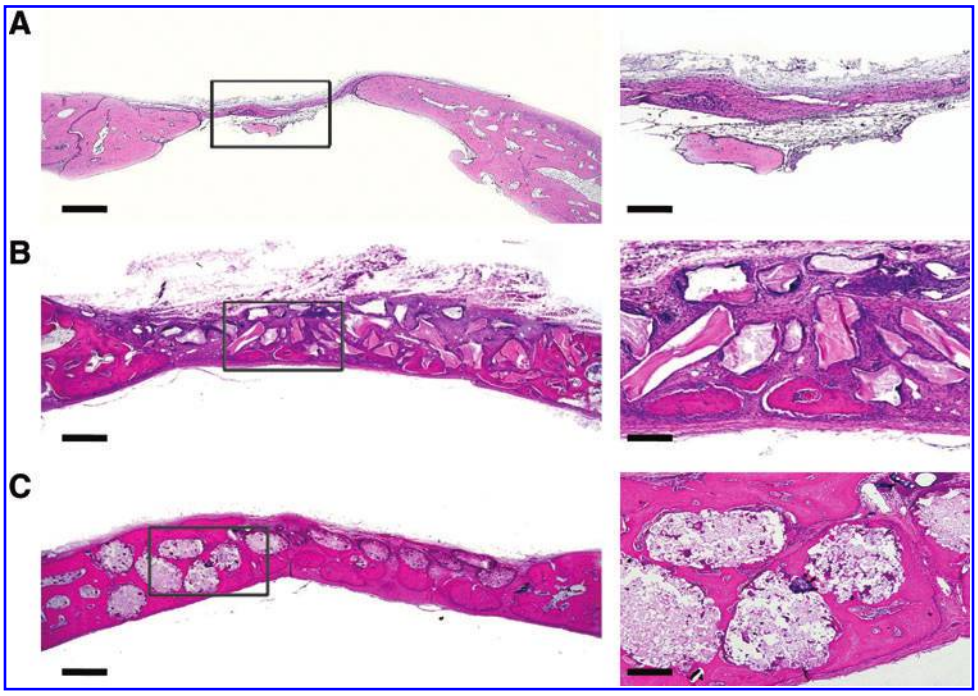

FIG. 3. Photomicrographs of the calvarial critical-sized bone defects in New Zealand white rabbits after bone regeneration for 4 weeks: (**A**) control, (**B**) Bio-OSS, and (**C**) MGSB. Scale bars: left, 1000 μm; right, 200 μm. Color images available online at www.liebertonline.com/ten.

According to our preliminary study, HA hydrogels alone were not effective for bone regeneration. In addition, highly stable HA-ADH hydrogels longer than 6 months and highly swelling HA-DVS hydrogels were not effective for bone regeneration despite using bone grafts together (Fig. 4A, B). Figure 4C and D show the histological photomicrographic images of calvarial critical-sized bone defects after bone regeneration by Bio-OSS/HA-CYS hydrogels and MGSB/HA-CYS hydrogels. Newly formed bone tissues by Bio-OSS/HA-CYS hydrogels were poorly integrated with Bio-OSS (Fig. 4C), whereas the regenerated bone tissues by MGSB/HA-CYS hydrogels were well interconnected with MGSB, showing a lamella bone structure around the bone grafts (Fig. 4D). The new bone formation was quantified by histomorphometric analysis with a statistical analysis using *t*-tests. The bioactive MGSB (62.7% ± 3.8%) and MGSB/HA-CYS hydrogels (71.0% ± 4.4%) resulted in statistically better bone regeneration than Bio-OSS/HA-CYS hydrogels (44.7% ± 3.4%) ($p < 0.01$). The regenerated bone by MGSB/HA-CYS hydrogels in 4 weeks was as high as 43% and occupied 71% of the bone defect area with MGSB in the form of a calvarial bone plate. Figure 4E shows the bone regeneration by MGSB/HA-CYS hydrogels in 8 weeks. The synthetic bone graft of MGSB was bioabsorbed and replaced gradually by newly formed bone with increasing bone regeneration. According to histomorphometric analysis, the amount of bioabsorbed MGSB was estimated to be approximately 10.2% in 8 weeks.

X-ray imaging of bone regeneration by artificial bone substitutes

Synchrotron X-ray bioimaging was carried out to visualize the bone regeneration by artificial bone substitutes. Figure 5A shows a projection image of the critical-sized bone defect area after bone regeneration by the control for 4 weeks. The bone regeneration was not enough to cover the whole bone defect. To visualize the bone regeneration more clearly, tomographic cross-sectional image analysis was carried out for the regions in the squares illustrated in Figure 5A. The blue square (1.5×1.5 mm) was set near the bone defect boundary, the red one near the center of bone defect, and the yellow one continuous to the red, respectively (Fig. 5A). Figure 5B shows the vertical tomographic slice images around the three squares. The thickness of regenerated bone became narrow to the center of bone defects. Eventually, there was little bone regeneration at the center. In comparison with the control, the bone regeneration by Bio-OSS/HA-CYS hydrogels and MGSB/HA-CYS hydrogels was also analyzed by X-ray tomography. Figure 5C and D show the vertical tomographic slice images near the bone defect boundary after bone regeneration for 4 weeks. The newly formed bone plate had a uniform thickness on the tomographic image, reflecting simultaneous bone regeneration in the calvarial critical-sized bone defect region. HA-CYS hydrogels were not observed on the image and thought to have been degraded contributing for the bone regeneration. Compared with the case of Bio-OSS/HA-CYS hydrogels (Fig. 5C), the regenerated bone (blue arrowheads) by MGSB/HA-CYS hydrogels was well interconnected with MGSB (green arrowheads) regardless of the position in the bone defect area (Fig. 5D).

Figure 6 shows 3D reconstructed images of tomographic data for the critical-sized bone defects after bone regeneration by the artificial bone substitute samples for 4 weeks (Fig. 6A–C, E) and 8 weeks (Fig. 6D, F). The 3D volume-rendering image of the control in Figure 6A revealed that the regenerated bone had a porous structure with an empty inner part. In contrast, those of artificial bone substitutes showed micron-scale morphologies of regenerated bone plates (Fig. 6B–F). The synchrotron 3D X-ray images clearly confirmed that the bone regeneration by MGSB/HA-CYS hydrogels was the most effective, with an excellent integration of regenerated bones to the MGSB (Fig. 6E, F). Bio-OSS (green arrow) revealed smooth surface reflecting poor interconnection with

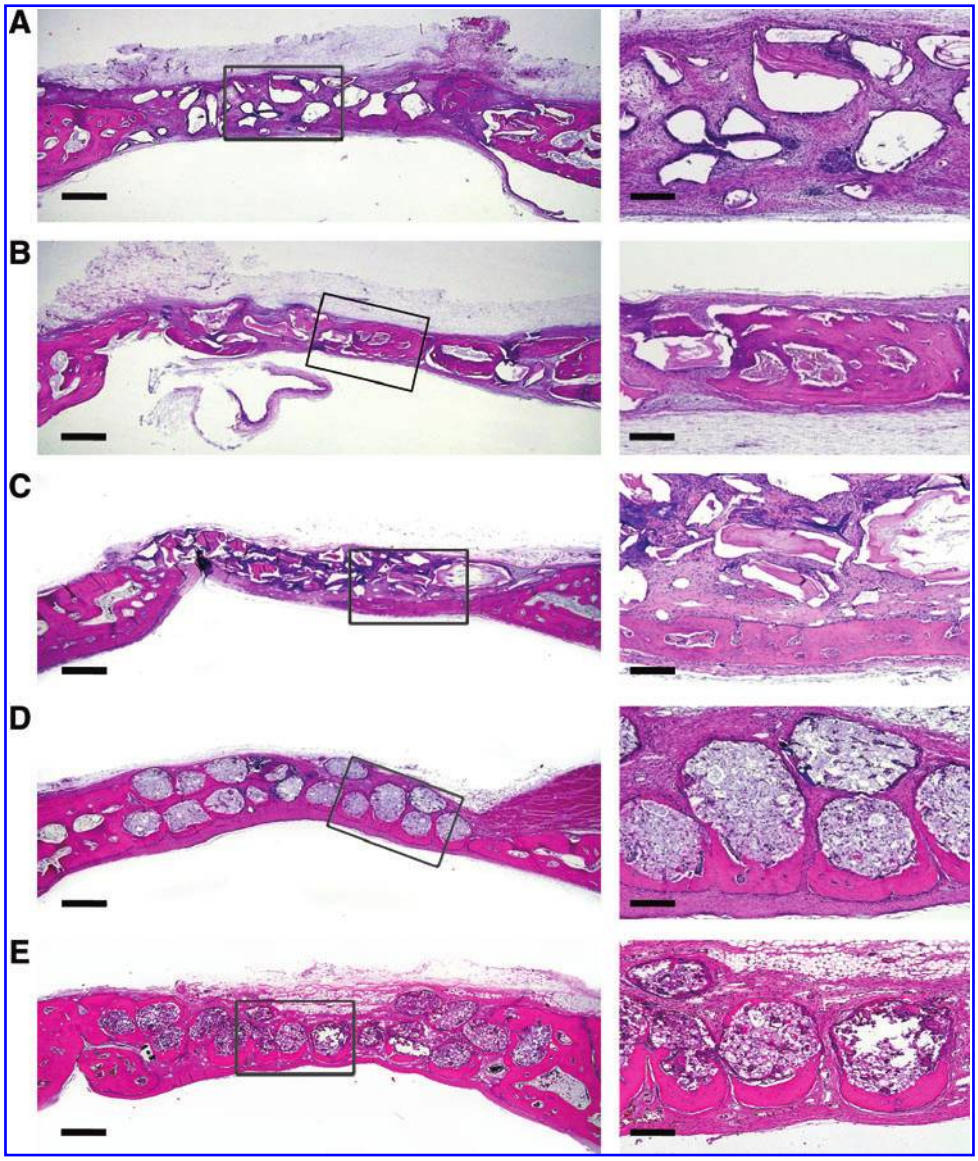

FIG. 4. Photomicrographs of the calvarial critical-sized bone defects in New Zealand white rabbits after bone regeneration for (**A–D**) 4 weeks and (**E**) 8 weeks: (**A**) Bio-OSS/HA-ADH hydrogels, (**B**) Bio-OSS/HA-DVS hydrogels, (**C**) Bio-OSS/HA-CYS hydrogels, and (**D, E**) MGSB/HA-CYS hydrogels. Scale bars: left, 1000 μm; right, 200 μm. Color images available online at www.liebertonline.com/ten.

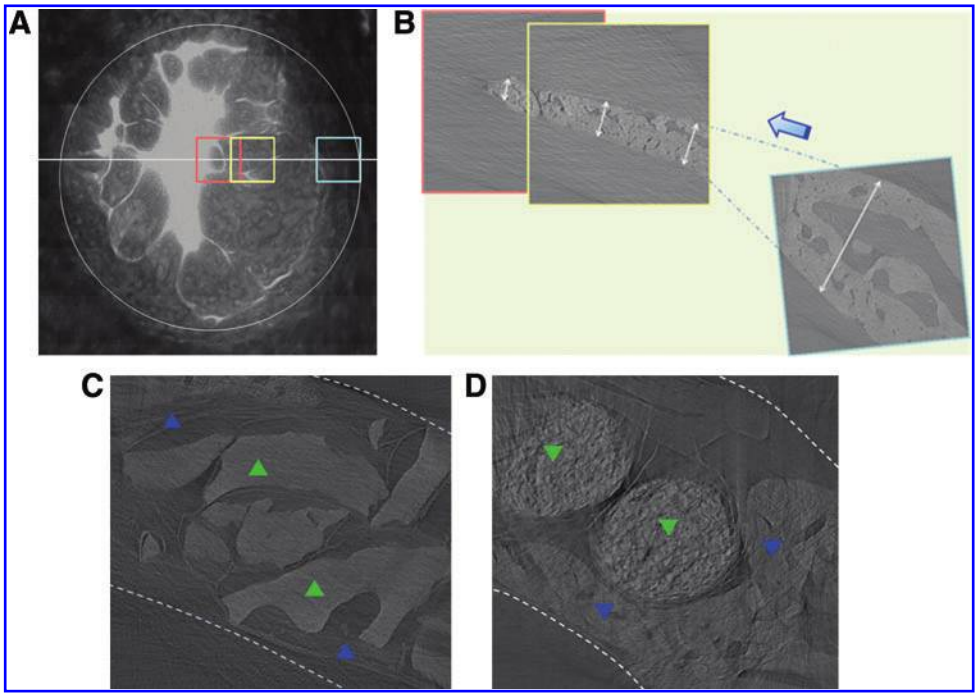

FIG. 5. Synchrontron X-ray tomographic images of the calvarial critical-sized bone defects in New Zealand white rabbits after bone regeneration by artificial bone substitutes for 4 weeks: (**A**) two-dimensional projection image of the bone defect area in the control group, (**B**) cross-sectional images around the red, yellow, and blue boxes in (**A**) showing continuous merged pictures of regenerated bones to the direction of white and blue arrows. (**C**) cross-sectional image of regenerated bones by Bio-OSS/HA-CYS hydrogels, and (**D**) that by MGSB/HA-CYS hydrogels. Green arrowheads indicate bone substitutes and blue arrowheads indicate regenerated bone. Color images available online at www.liebertonline.com/ten.

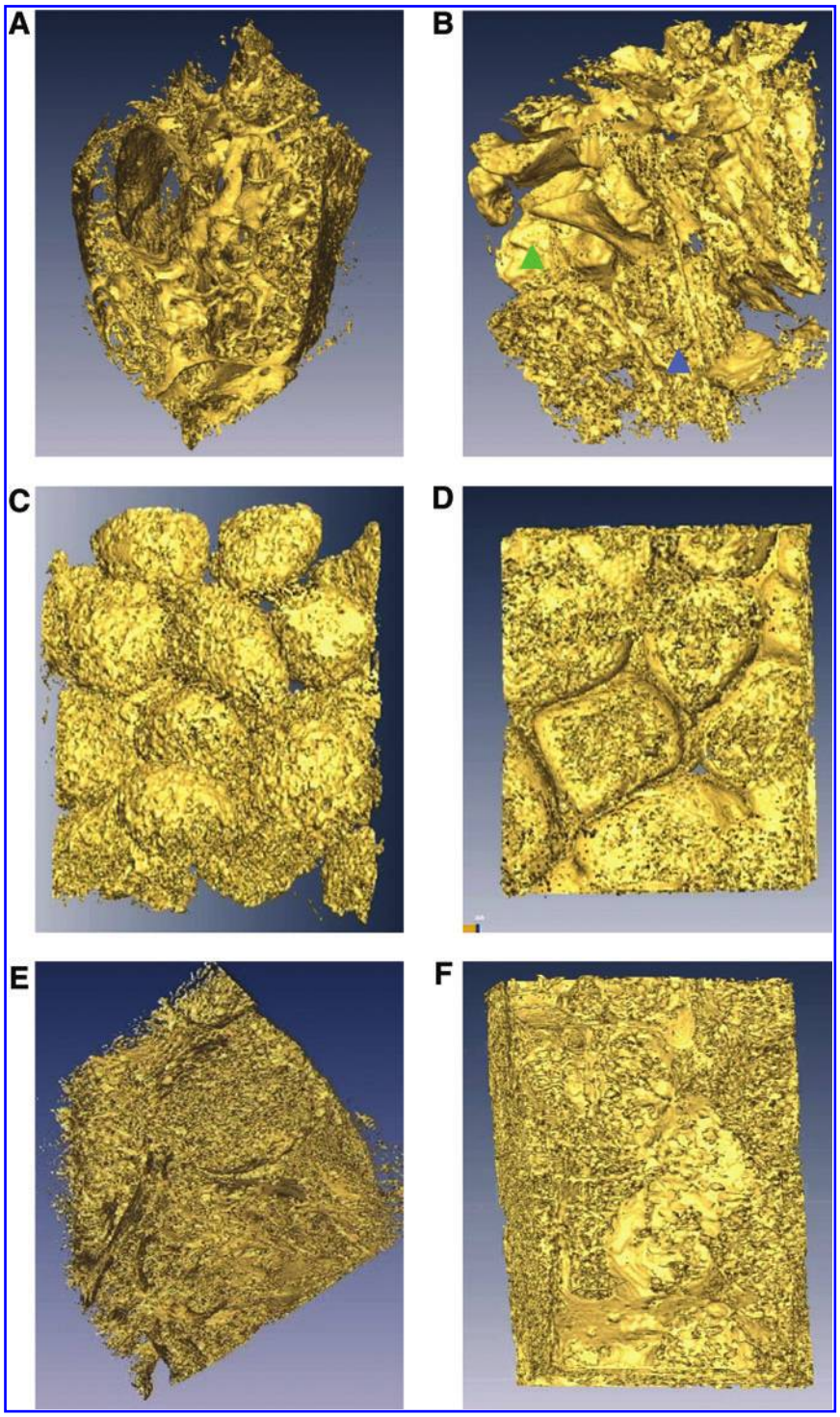

FIG. 6. Synchrontron X-ray three-dimensional reconstructed images of the calvarial critical-sized bone defects in New Zealand white rabbits after bone regeneration by artificial bone substitutes for (**A–C, E**) 4 weeks and (**D, F**) 8 weeks: (**A**) control, (**B**) Bio-OSS/HA-CYS hydrogels, (**C, D**) MGSB, and (**E, F**) MGSB/HA-CYS hydrogels. Green arrowhead indicates bone substitute and blue arrowhead indicates regenerated bone. Color images available online at www.liebertonline.com/ten.

the regenerated bones (blue arrow) by Bio-OSS/HA-CYS hydrogels (Fig. 6B). In addition, the bone regeneration by MGSB without HA-CYS hydrogels was not so much effective, exhibiting the remaining round morphology of MGSB (Fig. 6C, D). However, the bone regeneration by MGSB/HA-CYS hydrogels for 4 and 8 weeks resulted in mature and dense bone plate formation around MGSB (Fig. 6E, F). The 3D X-ray bioimaging videos of regenerated bones are available in Supplemental Materials (available online at www.liebertonline.com). Finally, the regenerated bones by MGSB/HA-CYS hydrogels were investigated in more detail by sequential nondestructive synchrotron X-ray tomographic analysis (Fig. 7). The results clearly showed that newly formed bone was tightly integrated with MGSB granules regardless of the position in the bone defect area of New Zealand white rabbits. The 2D tomographic transmission images from anterior to posterior of the samples were used for the determination of void volumes in the calvarial bone defect regions. The void volumes after treatments with the control, Bio-OSS/HA-CYS hydrogels, and MGSB/HA-CYS hydrogels in 4 weeks were 74.8%, 43.6%, and 33.7%, respectively. In other words, the regenerated bone plate volume by MGSB/HA-CYS

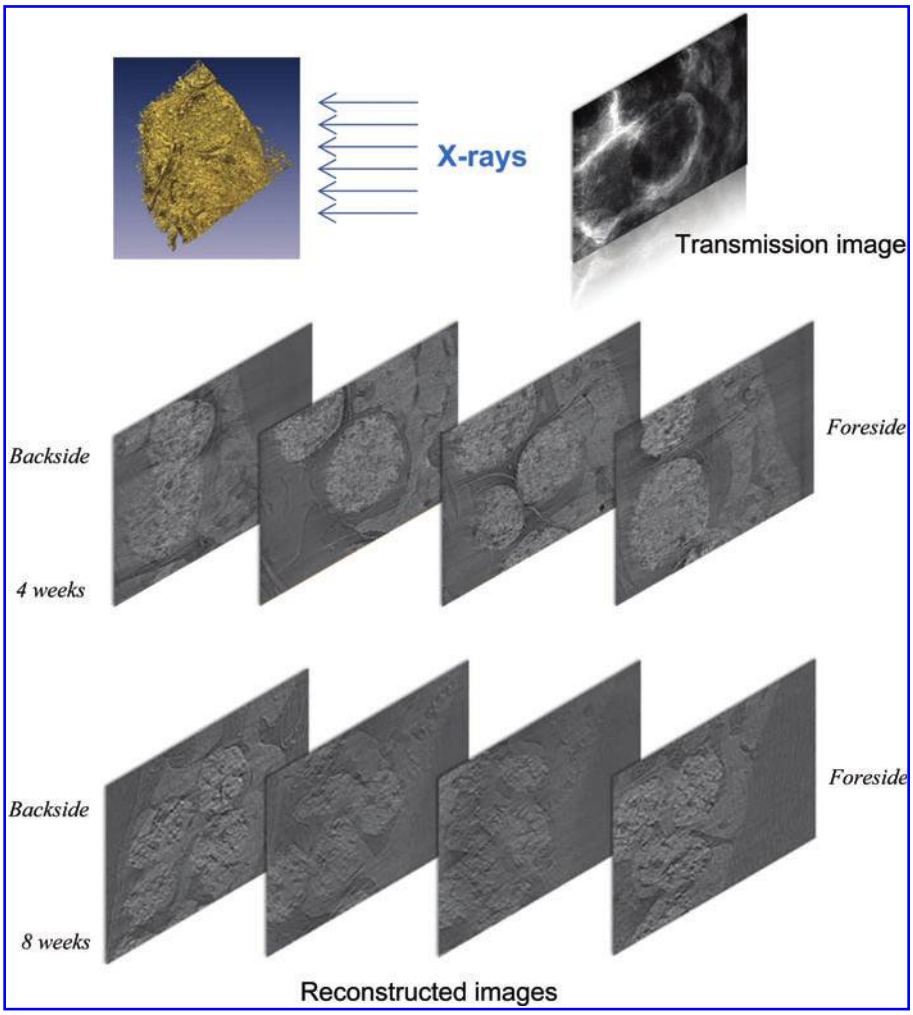

FIG. 7. Sequential synchrotron X-ray tomographic images of regenerated bones by MGSB/HA-CYS hydrogels in the calvarial critical-sized bone defects of New Zealand white rabbits after 4 and 8 weeks. Color images available online at www.liebertonline.com/ten.

hydrogels was approximately 66.3%, which was well matched with the histomorphometric analysis results.

Discussion

Many kinds of bone substitutes have been investigated, such as Bio-OSS, ceramic bone substitutes,[29] monetite granules,[26] deproteinized bone grafts,[30] and biodegradable poly (D,L-lactic acid) (PLA) scaffolds.[4] The regenerated bone volume by commercially available ceramic bone grafts was as high as 30–50% of the bone defect area in 3–6 weeks.[29] In case of vascular endothelial growth factor-encapsulated PLA seeded with MSCs, the regenerated bone volume was less than 30% in 4 weeks.[4] Although the attempts boosted local bone regeneration for 4 weeks, the rapid bone plate formation was not possible without ceramic bone grafts. In addition, the approach might not be feasible for clinical applications because of the high production cost of bone-related growth factors such as BMP and vascular endothelial growth factor, the safety issues of MSCs, and so on.

In this work, an artificial bone substitute of MGSB and HA hydrogels was prepared and assessed in the calvarial critical-sized bone defects of New Zealand white rabbits. The composition of MGSB was 60 wt% of hydroxyapatite and 40 wt% of β-TCP, which was known to be the best in terms of biodegradability and mechanical strength for bone regeneration.[27,28] As well known, Bio-OSS, prepared by mechanical pulverization of bovine bone, has smooth surface and sharp edges. These physical characteristics might result in the thick fibrous encapsulation of Bio-OSS at the end of the wound healing stage. The degree of fibrous tissue formation surrounding implant materials was reported to depend on their surface topography.[16] The fibrous capsules, generated by the host, isolate the bone grafts from the biological milieu.[31] On the other hand, HA-CYS hydrogels with cleavable disulfide bonds were prepared and compared with HA-ADH and HA-DVS hydrogels. The swelling ratio of HA-DVS hydrogels by the crosslinking of HA-OH was significantly higher than those of other HA-ADH and HA-CYS hydrogels by the crosslinking of HA-COOH. HA hydrogels with a high swelling ratio might be inadequate for bone regeneration occupying the bone defect area. In addition, highly stable HA-ADH hydrogels[22,23] were also thought not to be adequate for bone regeneration without HA supply during the bone regeneration. Despite the chemical modification of carboxyl groups, HA-CYS hydrogels degraded rapidly because of the cleavable crosslinkers containing disulfide bonds. Glutathione is known to reduce disulfide bonds acting as an electron donor. The different degradation behaviors of HA-CYS hydrogels by hyaluronidase and glutathione might be attributed to the different degradation mechanisms (Fig. 2). Glutathione cleaves the disulfide bond on the

crosslinker, whereas hyaluronidase acts somewhere on the multiple repeating units on HA backbone. Both hyaluronidase and glutathione are present in the body, which can affect the degradation of HA hydrogels. However, we could not carry out *in vitro* degradation tests using both hyaluronidase and glutathione, because glutathione deactivates hyaluronidase by disulfide bond cleavage.[16] As we previously reported elsewhere, HA hydrogels containing disulfide bonds like HA-CYS hydrogels degraded almost completely in the subcutaneous tissue in a month.[22,23,32]

Among the seven different samples, a control, Bio-OSS, MGSB, Bio-OSS/HA-ADH hydrogels, Bio-OSS/HA-DVS hydrogels, Bio-OSS/HA-CYS hydrogels, and MGSB/HA-CYS hydrogels, MGSB/HA-CYS hydrogels resulted in the most effective bone regeneration. HA-CYS hydrogels in the artificial bone substitutes facilitated their fixation to the bone defect area. The biodegradable and biocompatible MGSB appeared to be advantageous over Bio-Oss in terms of regenerated bone volume and its interconnection with the regenerated bones. A uniform spherical morphology of MGSB with a microporous structure appeared to be advantageous for osteoblast cell adhesion and proliferation. HA-CYS hydrogels with a degradation period of approximately 1 month contributed for effective bone regeneration, promoting the infiltration of osteoblasts by the provision of osteoconductive and angiogenic HA in the early stage of bone regeneration. The bone regeneration by MGSB/HA-CYS hydrogels was as high as 43% and occupied 71% of the bone defect area with MGSB in the form of a calvarial bone plate in 4 weeks. The BCP of MGSB with 60 wt% hydroxyapatite and 40 wt% β-TCP was biodegraded, bioabsorbed, and replaced gradually by newly formed bone with increasing bone regeneration. The histomorphometric analysis revealed that the amount of bioabsorbed MGSB was approximately 10.2% in 8 weeks, which might be ascribed mainly to the biodegradation of β-TCP. The bioabsorption ratios of hydroxyapatite and β-TCP in 12 weeks were reported to be approximately 2% and 34%, respectively.[33] The remaining hydroxyapatite was integrated with regenerated bone without causing any adverse effects.[33] Bone is known to be regenerated by calcium phosphate deposition of osteoblast after the formation of extracellular matrix.[34]

The bone regeneration by the artificial bone substitutes was visualized by synchrotron X-ray bioimaging. The microtomographic experimental geometry and the detector position for the 7B2 synchrotron X-ray microscopy were selected to emphasize the refraction-based mechanism.[24,25] The bone regeneration by the control proceeded from the boundary of bone defect area to the inside, whereas that by the Bio-OSS/HA-CYS hydrogels and MGSB/HA-CYS hydrogels occurred throughout the bone defect area. The inner part of regenerated bone by the control around the boundary was empty reflecting cancellous bone formation after 4 weeks. As shown in 2D and 3D X-ray tomographic images, the regenerated bone by MGSB/HA-CYS hydrogels was tightly interconnected with MGSB (Figs. 5–7). The woven bone structure filling the entire bone defect area was well matured to the lamellar bone structure around the partially bioabsorbed MGSB. Videos found in Supplemental Materials show the 3D morphologies of regenerated bones more clearly. The sequential nondestructive synchrotron X-ray tomographic analysis from anterior to posterior of the samples also confirmed the effective bone regeneration by MGSB/HA-CYS hydrogels matching with the histomorphometric analysis results. The novel X-ray imaging would be successfully exploited to investigate the bone regeneration process *in vivo* as a nondestructive method and contribute for the development of artificial bone substitutes for clinical applications.

In conclusion, a clinically feasible artificial bone substitute consisted with MGSB and HA hydrogels was successfully developed for bone tissue engineering applications. The bioactive BCP of MGSB was prepared by the chemical precipitation method to have a composition with 60 wt% of hydroxyapatite and 40 wt% of β-TCP. HA-CYS hydrogels with cleavable disulfide linkages were prepared to supply HA continuously for effective bone regeneration by their controlled degradation *in vivo*. Among artificial bone substitutes tested in this work, MGSB/HA-CYS hydrogels implanted in the calvarial critical-sized bone defects of New Zealand white rabbits resulted in the most effective bone regeneration. The bone regeneration by MGSB/HA-CYS hydrogels was as high as 43% and occupied 71% of the bone defect area with MGSB in the form of a calvarial bone plate. MGSB was biodegraded, bioabsorbed, and replaced gradually by newly formed bones, with increasing bone regeneration as observed in 8 weeks. Further, synchrotron X-ray imaging clearly confirmed the effective bone regeneration by MGSB/HA-CYS hydrogels, showing 3D micron-scale morphologies of regenerated bones being interconnected with MGSB. The sequential nondestructive synchrotron X-ray tomographic analysis of void volume after bone regeneration also confirmed the effective bone regeneration by MGSB/HA-CYS hydrogels. The novel MGSB/HA-CYS hydrogel system will be investigated further for clinical applications using synchrotron X-ray bioimaging.

Acknowledgments

This study was supported by a grant from the Korea Health 21 R&D Project, Ministry of Health and Welfare, Republic of Korea (A060412, A084132) and by the Creative Research Initiatives (Functional X-ray Imaging) of MEST/KOSEF.

Disclosure Statement

No competing financial interests exist.

References

1. Stevens, M., Marini, R., Schaefer, D., Aronson, J., Langer, R., and Shastri, V. *In vivo* engineering of organs: the bone bioreactor. Proc Natl Acad Sci USA **102,** 11450, 2005.
2. Chu, T., Warden, S., Turner, C., and Stewart, R. Segmental bone regeneration using a load-bearing biodegradable carrier of bone morphogenetic protein-2. Biomaterials **28,** 459, 2007.
3. Jung, R., Weber, F., Thoma, D., Ehrbar, M., Cochran, D., and Hammerle, C. Bone morphogenetic protein-2 enhances bone formation when delivered by a synthetic matrix containing hydroxyapatite/tricalciumphosphate. Clin Oral Implants Res **19,** 188, 2008.
4. Kanczler, J., Ginty, P., Barry, J., Clarke, N., Howdle, S., Shakesheff, K., and Oreffo, O. The effect of mesenchymal populations and vascular endothelial growth factor delivered from biodegradable polymer scaffolds on bone formation. Biomaterials **29,** 1892, 2008.
5. Kim, J., Kim, I., Cho, T., Lee, K., Hwang, S., Tae, G., Noh, I., Lee, S., Park, Y., and Sun, K. Bone regeneration using hyaluronic

acid-based hydrogel with bone morphogenic protein-2 and human mesenchymal stem cells. Biomaterials **28,** 1830, 2007.
6. Merkx, M., Maltha, J., Freihofer, H., and Kuijpers-Jagtman, A. Incorporation of particulated bone implants in the facial skeleton. Biomaterials **20,** 2029, 1999.
7. Gauthier, O., Goyenvalle, E., Bouler, J., Guicheux, J., Pilet, P., Weiss, P., and Daculsi, G. Macroporous biphasic calcium phosphate ceramics versus injectable bone substitute: a comparative study 3 and 8 weeks after implantation in rabbit bone. J Mater Sci Mater Med **12,** 385, 2001.
8. Aebli, N., Stichm, H., Schawalder, P., Theis, J., and Krebs, J. Effects of bone morphogenetic protein-2 and hyaluronic acid on the osseointegration of hydroxyapatite-coated implants: an experimental study in sheep. J Biomed Mater Res A **73,** 295, 2005.
9. Dawson, J., and Oreffo, R. Bridging the regeneration gap: stem cells, biomaterials and clinical translation in bone tissue engineering. Arch Biochem Biophys **473,** 124, 2008.
10. Chang, S., Chuang, H., Chen, Y., Yang, L., Chen, J., Mardini, S., Chung, H., Lu, Y., Ma, W., and Lou, J. Cranial repair using BMP-2 gene engineered bone marrow stromal cells. J Surg Res **119,** 85, 2004.
11. Carano, R., and Filvaroff, E. Angiogenesis and bone repair. Drug Discov Today **8,** 980, 2003.
12. Street, J., Bao, M., deGuzman, L., Bunting, S., Peale, F., Jr., Ferrara, N., Steinmetz, H., Hoeffel, J., Cleland, J., Daugherty, A., van Bruggen, N., Carano, R., and Filcaroff, E. Vascular endothelial growth factor stimulates bone repair by promoting angiogenesis and bone turnover. Proc Natl Acad Sci USA **99,** 9656, 2002.
13. Wang, Y., Wan, C., Deng, L., Liu, X., Cao, X., Gilbert, S., Bouxsein, M., Faugere, M., Guldberg, R., Gerstenfeld, L., Haase, V., Johnson, R., Schipani, E., and Clemens, T. The hypoxia-inducible factor alpha pathway couples angiogenesis to osteogenesis during skeletal development. J Clin Invest **117,** 1616, 2007.
14. Yoshikawa, M., Tsuji, N., Toda, T., and Ohgushi, H. Osteogenic effect of hyaluronic acid sodium salt in the pores of a hydroxyapatite scaffold. Mater Sci Eng C **27,** 220, 2007.
15. Denlinger, J. Hyaluronan and its derivatives as vis-coelastics in medicine. In: Laurent, T.C., and Balazs, E.A., eds. Chemistry, Biology and Medical Applications of Hyaluronan and its Derivatives. London, UK: Potland Press, 1998, pp. 235–242.
16. Chao, K., Muthukumar, L., and Herzberg, O. Structure of human hyaluronidase-1, a hyaluronan hydrolyzing enzyme involved in tumor growth and angiogenesis. Biochemistry **46,** 6911, 2007.
17. Slevin, M., Kumar, S., and Gaffney, J. Angiogenic oligosaccharides of hyaluronan induce multiple signaling pathways affecting vascular endothelial cell mitogenic and wound healing responses. J Biol Chem **277,** 41046, 2002.
18. Fraser, J., Kimpton, W., Laurent, T., Cahill, R., and Vakakis, N. Uptake and degradation of hyaluronan in lymphatic tissue. Biochem J **256,** 153, 1988.
19. Kim, J., Park, K., and Hahn, S. Effect of hyaluronic acid molecular weight on the morphology of quantum dot-hyaluronic acid conjugates. Int J Biol Macromol **42,** 41, 2008.
20. Laurent, T., Dahl, I., Dahl, L., Engstrom-Laurent, A., Eriksson, S., Fraser, J.R., Granath, K., Laurent, C., Laurent, U., Lilja, K., Pertoft, H., Smedsrod, B., Tengblad, A., and Wik, O. The catabolic fate of hyaluronic acid. Connect Tissue Res **15,** 33, 1986.
21. Smedsr, B.D. Cellular events in the uptake and degradation of hyaluronan. Adv Drug Deliv Rev **7,** 265, 1991.
22. Oh, E., Kang, S., Kim, B., Jiang, G., Cho, I., and Hahn, S. Control of the molecular degradation of hyaluronic acid hydrogels for tissue augmentation. J Biomed Mater Res A **86,** 685, 2008.
23. Hahn, S., Park, J., Tomimatsu, T., and Shimoboji, T. Synthesis and degradation test of hyaluronic acid hydrogels. Int J Biol Macromol **40,** 374, 2007.
24. Baik, S., Kim, H., Jeong, M., Lee, C., Je, J., Hwu, Y., and Margaritondo, G. International consortium on phase contrast imaging and radiology beamline at the Pohang Light Source. Rev Sci Instrum **75,** 4355, 2004.
25. Hwu, Y., Tsai, W., Je, J., Seol, S., Kim, B., Groso, A., Margaritondo, G., Lee, K., and Seong, J. Synchrotron microangiography with no contrast agent. Phys Med Biol **49,** 501, 2004.
26. Tamimi, F., Torres, J., Kathan, C., Baca, R., Clemente, C., Blanco, L., and Cabarcos, E. Bone regeneration in rabbit calvaria with novel monetite granules. J Biomed Mater Res A **87,** 980, 2008.
27. Daculsi, G., Passuti, N., Martin, S., Deudon, C., Legeros, R., and Raher, S. Macroporous calcium phosphate ceramic for long bone surgery in humans and dogs. Clinical and histological study. J Biomed Mater Res **24,** 379, 1990.
28. Gauthier, O., Bouler, J., Aguado, E., Pilet, P., and Daculsi, G. Macroporous biphasic calcium phosphate ceramics: influence of macropore diameter and macroporosity percentage on bone ingrowth. Biomaterials **19,** 133, 1998.
29. Hing, K., Wilson, L., and Buckland, T. Comparative performance of three ceramic bone graft substitutes. Spine J **7,** 475, 2007.
30. Kousuke, O., Yoshinaka, S., Hui, X., and Kiyoshi, O. Blood-filled spaces with and without deproteinized bone grafts in guided bone regeneration: a histomorphometric study of the rabbit skull using non-resorbable membrane. Clin Oral Implants Res **16,** 236, 2005.
31. Kay, C., David, A.P., and Rena, B. An Introduction to Tissue-Biomaterial Interactions. Hoboken, New Jersey: WILEY-LISS, 2002.
32. Hahn, S., Kim, J., and Shimobouji, T. Injectable hyaluronic acid microhydrogels for controlled release formulation of erythropoietin. J Biomed Mater Res A **80,** 916, 2007.
33. Lu, J., Descamps, M., Dejou, J., Koubi, G., Hardouin, P., Lemaitre, J., and Proust, J. The biodegradation mechanism of calcium phosphate biomaterials in bone. J Biomed Mater Res **63,** 408, 2002.
34. Boskey, A. Matrix proteins and mineralization: an overview. Connect Tissue Res **35,** 357, 1996.

Address correspondence to:
Sei Kwang Hahn, Ph.D.
Department of Material Science and Engineering
Pohang University of Science and Technology (POSTECH)
San 31, Hyoja-dong, Nam-gu
Pohang 790-784
Korea

E-mail: skhanb@postech.ac.kr

Jung Ho Je, Ph.D.
Department of Material Science and Engineering
Pohang University of Science and Technology (POSTECH)
San 31, Hyoja-dong, Nam-gu
Pohang 790-784
Korea

E-mail: jhje@postech.ac.kr

Received: November 25, 2009
Accepted: January 14, 2010
Online Publication Date: February 17, 2010